

Hybrid Evolutionary Ridge Regression Approach for High-Accurate Corner Extraction

Gustavo Olague, Benjamín Hernández and Enrique Dunn
EvoVisión Project *, Computer Science Department
CICESE, Research Center, Applied Physics Division
Ensenada, B.C., México.

Abstract

Corner measurement is of main concern within the following tasks: camera calibration, image matching, object tracking, recognition and reconstruction. This paper presents a hybrid evolutionary ridge regression approach for the problem of corner modeling. We search model parameters characterizing L-corner models by means of fitting the model to the image data. As the model fitting relies on an initial parameter estimation, we use a global approach to find the global minimum. Experimental results applied to an L-corner using several levels of noise show the advantages and disadvantages of our evolutionary algorithm compared to down-hill simplex and simulated annealing.

1. Introduction and Motivation

Computer vision can be understood as the science of obtaining reliable, accurate and useful information from images in order to execute and complete tasks devoted to perceiving, sensing and interacting with the world around a machine vision system. A common paradigm to computer vision is the extraction of features described by specialized criteria depending on the task at hand. Feature extraction is one of the most important areas in computer vision. A great deal of effort has been spent by the computer vision community on this problem, see [1], [25], [11] and in particular on the problem of edge detection, see [17], [5], [4], [6]. Corner extraction follows a number of approaches which can be broadly divided into two categories: boundary based approaches and gray scale approaches. Boundary based approaches detect corners on the boundaries of objects. The boundary or contour based methods involves, first, segmenting a scene image into meaningful regions, then extracting boundaries from the regions of interest to finally search for maximal curvature or inflexion points along the contour, see [18], [24]. The second group consists of approaches that work directly on a gray level image. Several techniques

have been proposed within this group. These techniques cover heuristic approaches like the “interest operator” of Moravec [19], or through the gradient computing [3] [10], [14]. Parametric model based methods are considered as a gray level approach as long as they work directly with the gray level image. Parametric model based methods can be traced back to the photogrammetric literature [12]. The basic idea is to propose a parametric model and then fitting the model directly to image intensities, see [22], [8], [2] [15]. Deriche and Giraudon approach [7], is based on differential geometric measures of curvature such as the determinant of the Hessian or the second directional derivative orthogonal to the gradient. In order to improve the precision in localization, for each detected local maxima they fit a quadratic surface around each local maxima obtaining subpixel precision. In general, all approaches consider the proposed model as defined by a unit step function which is convolved with a Gaussian followed by an affine or euclidean transformation. However, our approach is motivated by the idea of avoiding the two step process of convolving the proposed model with a Gaussian. Instead of it, we work with a model that directly takes into account the level of blurring found in bandlimited systems like the CCD cameras [15]. Another problem is that the quality of the approximation depends on the initial position estimation. Indeed, parametric model based approaches are suitable for high accurate localization. However, there are not any studies about which kind of approach is suitable for improving the accuracy while eliminating the problem of initial parameters’ estimation. This paper presents first results on three different algorithms that use a local criteria for measuring the L-corner position.

2 L-Corner Modeling

Modeling image intensities of an L-corner to a model ($f(x_i, y_i), x_i, y_i$) that is a linear combination of nonlinear functions of (x_i, y_i) is a subject known as modeling of data. In our previous work we have introduced the Unit Step Edge Function (USEF) as a fundamental component in multi-

*This research was supported by CONACyT-INRIA through the LAFMI project.

corner modeling [15]. An L-corner is built of two USEF using the error function as follows:

Definition 1 (Error Function) *The error function, also called Gaussian probability integral, is a special case of the incomplete gamma function, and is obtained directly from C compilers. Its definition is:*

$$erf(x) = \frac{2}{\sqrt{\pi}} \int_0^x e^{-t^2} dt \quad (1)$$

The function has the following limiting values and symmetries:

$$erf(0) = 0 \quad erf(\infty) = 1 \quad erf(-x) = -erf(x)$$

According to the above definition we can derive a new function dividing the error function by 2 and adding half of a Normal distribution in order to obtain a distribution function as follows:

$$F(x) = \frac{1}{\sqrt{\pi}} \int_0^x e^{-t^2} dt + \frac{1}{\sqrt{2\pi}} \int_{-\infty}^0 e^{-\frac{1}{2}t^2} dt = \frac{erf(x)}{2} + \frac{1}{2}$$

by replacing x appropriately we can derive the USEF definition along the x -axis.

Definition 2 (Unit Step Edge Function) *Let the image coordinates and the set of unknown model parameters be denoted by $I = (x, y)$ and $P_x = (p_{x1}, \dots, p_{xn})$ respectively. The unit step edge function is represented as follows:*

$$U_x(I, P_x) = \pm \frac{1}{\sigma_1 \sqrt{2\pi}} \int e^{-\frac{(t-y \cdot \tan(\theta_1) - \mu_1)^2}{2\sigma_1^2}} dt + \frac{1}{2} \quad (2)$$

Where the image coordinates range from $[-m, m]$. The central point μ_1 designs the position x of the line that crosses along the y -axis. μ_1 ranges from $[-m, m]$. The rotation θ_1 is made clockwise about the (positive) y -axis. θ_1 designs the orientation of the edge model to be fitted to the image within the range $-\frac{\pi}{2} < \theta_1 < \frac{\pi}{2}$. Finally a scaling factor σ_1 that characterizes the amount of blur introduced by the discretization process needs to be taken into account. σ_1 ranges from $[0, m]$. The unit edge function describes a distribution function that increases steadily from 0 to 1 with respect to the x -axis. The unit step edge function $U_y(I, P_y)$ with respect to the y -axis is represented in a similar way, where all intervals of the variables remain the same. $U_y(I, P_y)$ can be evaluated numerically using the Gaussian error function as follows:

$$U_y(I, P_y) = \pm \frac{1}{2} erf \left(\frac{\sqrt{2}(-x + y \cdot \tan(\theta_2) + \mu_2)}{2\sigma_2} \right) + \frac{1}{2} \quad (3)$$

Note that the variable of integration is now y . In order to obtain an L-corner model we multiply both USEF as follows:

$$M_L^t(x, y, \vec{P}) = U_x(I, P_x) \cdot U_y(I, P_y) \cdot A + B \quad (4)$$

The parameters $\sigma_1, \theta_1, \mu_1, \sigma_2, \theta_2, \mu_2, A$ y B , represents the physical and geometrical contours of an L-corner.

3 Global Model Fitting

In general an optimization problem requires finding a set of $\vec{P} \in S$, where S is a bounded set on \mathcal{R}^n , such that a certain quality criterion $f : S \rightarrow \mathcal{R}$, typically called the objective function is minimized or equivalently maximized. Without loss of generality, it is sufficient to consider only minimization tasks, since maximizing $f()$ is equivalent to minimizing $-f()$. The problem then is to find a point $\vec{P}_{\min} \in S$ such that $f(\vec{P}_{\min})$ is a global minimum on S . More specifically, it is required to find an $\vec{P}_{\min} \in S$ such that

$$\forall \vec{P} \in S : f(\vec{P}_{\min}) \leq f(\vec{P}).$$

The above analysis suggests that a global optimization technique can be used to solve the problem of initial parameters' estimation. Experimental science is devoted to fitting a model that depends on adjustable parameters to a given set of observations. The common approach is to select or design a merit function that measures the agreement between the data and the model with a particular choice of parameters. The model parameters are then adjusted to achieve a minimum in the merit function, yielding a set of best-fit-parameters. The adjustment process is basically a problem of minimization in many dimensions. Finding the set of parameters that takes the function to a minimum or a maximum value is considered as an optimization problem. The task of maximization and minimization are trivially related to each other as one being the inverse of the other. An extremum (maximum or minimum) can be either global, truly the best solution, or local, the best around a neighborhood. Finding a global extremum is, in general, a very difficult problem. Moreover, in fitting data usually the merit function is not unimodal, with a single minimum, which makes the problem harder. On the other hand, there are important issues that are beyond the mere finding of best fit parameters. Data are generally not exact! Data are subject to measurement errors. Thus, typical data never fit exactly the model that is being used, even when the model is correct. It is customary to assume that the measurements are independent random variables. Each measurement ($f(x_i, y_i), x_i, y_i$) having a mean and a standard deviation. Fitting such a model to the data is carried out through

the well-known technique of least squares. The approach is to define a χ^2 merit function and determine best fit parameters by its minimization. Because of non-linearities, the minimization should proceed iteratively. Initial parameters' estimation is overcome through a global minimization estimation using the process of trial solution iteratively until χ^2 stops, or effectively stops, decreasing. Hence, our approach is to apply a global optimization technique using the least squares method as a local process in order to improve the search of the global optimum. As a by product of the minimization the covariances of the parameters should be obtained.

3.1 Modeling of Data and Multidimensional Optimization

The localization of a corner is obtained by fitting our parametric model to the image intensities. Estimates for the model parameters $\vec{P} = (p_1, \dots, p_n) \in \mathbb{R}^2$ are found by minimizing the squared differences between the (nonlinear) model function and the considered gray values:

$$Q = \chi^2 = F(\vec{P}) = \sum_{i=1}^m \sum_{j=1}^m \left[I(u_i, v_j) - M'_L(x_i, y_j, \vec{P}) \right]^2 \quad (5)$$

The intensities and the function values of the model in the considered image area are $I(u_i, v_j)$ and $M'_L(x_i, y_j, \vec{P})$ respectively. Previous approaches used by Rohr (1992) applied the method of Powell utilizing only function values or used the method of Levenberg-Marquardt, see [16] and [21], incorporating partial derivatives of the model function in order to reduce the computation time. However, a drawback presented on previous approaches is that the identification result relies on the initial parameter values and, as usual with nonlinear cost functions, in general we cannot guarantee to find the global minimum. This problem is overcome in this work using an hybrid evolutionary-ridge regression algorithm. In summary, n is the number of parameters to minimize in our model, while $m = 2w + 1$ defines the size of the input data. $\vec{P} = (\sigma_1, \mu_1, \theta_1, \sigma_2, \mu_2, \theta_2, A, B)$ are the parameters of M'_L that describe the behaviour of our L-corner. $M'_L(x_i, y_j, \vec{P})$ is the corner model evaluated at the \vec{P} parameters on the model coordinate system. $I(u_i, v_j)$ are the intensity values of an image in a gray scale, which is a square subimage of size $m \times m$ pixels within the entire image. $F(\vec{P})$ is the χ^2 estimator. The Equation (5) includes two different coordinate systems. The image coordinate system (u, v) and the model coordinate system (x, y) .

3.2 A Novel Evolutionary Representation

Evolutionary algorithms have risen as a rich paradigm for global optimization. Previous methodologies as the *Down*

Hill Simplex Method [20] and *Simulated Annealing* [13] are well known techniques for multidimensional optimization [21]. This section is devoted to our affine evolutionary algorithm for global optimization. Currently, evolutionary algorithms for numerical optimization use real code parameters for which a set of special transformations has been developed. The operations of crossover and mutation can be encapsulated into a single complex transformation as follows: We represent the actual points of the affine plane by pairs of non-homogeneous coordinates $Y = (Y_1, Y_2)$, where

$$Y_1 = \frac{y_1}{y_0}, Y_2 = \frac{y_2}{y_0}$$

The allowable representations \mathcal{R}_A of the affine plane are those representations \mathcal{R} of \hat{S}_2 in which the line i has the equation $y_0 = 0$; and this leads at once to the following theorem:

Theorem 1 *If \mathcal{R}_A is any allowable representation of the affine plane, then the whole class (\mathcal{A}) of allowable representations consists of all those representations, which can be derived from \mathcal{R}_A by applying a transformation of the form*

$$\begin{aligned} Y'_1 &= b_{11}Y_1 + b_{12}Y_2 + C_1 \\ Y'_2 &= b_{21}Y_1 + b_{22}Y_2 + C_2 \end{aligned}$$

where the coefficients are arbitrary real numbers, subject to the condition $|b_{rs}| \neq 0$.

Using Theorem 1, it is possible to transform the n variables of two solutions into a new pair of solutions, according to the following transformation:

$$\begin{pmatrix} Y'_{1_1} & Y'_{1_2} & \dots & Y'_{1_n} \\ Y'_{2_1} & Y'_{2_2} & \dots & Y'_{2_n} \end{pmatrix} = \begin{bmatrix} \underbrace{b_{11} \quad b_{12}}_{\text{crossover}} & \underbrace{C_1}_{\text{mutation}} \\ \underbrace{b_{21} \quad b_{22}}_{\text{crossover}} & \underbrace{C_2}_{\text{mutation}} \end{bmatrix}_n \begin{pmatrix} Y_{1_1} & Y_{1_2} & \dots & Y_{1_n} \\ Y_{2_1} & Y_{2_2} & \dots & Y_{2_n} \\ 1 & 1 & \dots & 1 \end{pmatrix} \quad (6)$$

Equation 6, can be expanded to the whole population. The advantages of this representation are:

1. Standardized treatment of all transformations.
2. Complex transformations are composed from single transformations by means of matrix multiplication.
3. An n dimensional point can be transformed by applying a set of n transformations.
4. Simple inversion of the transformation by matrix inversion.
5. Extremely fast, hardware supported matrix operations in high-power graphic workstations.

4 Experimental results

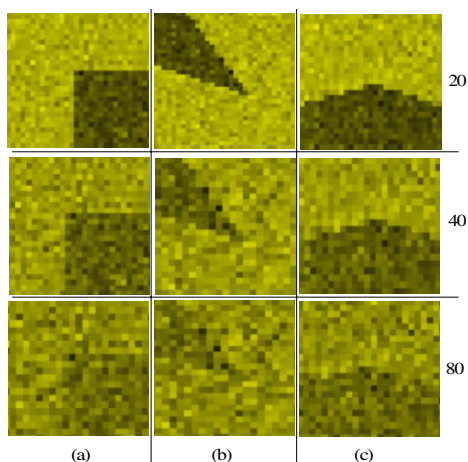


Figure 1: Structures (a), (b) and (c) of the test synthetic image with Gaussian noise scaled by $\lambda = 20, 40, 80$.

In order to show the robustness of each algorithm and the stability of our L-corner model, we applied Gaussian noise of zero mean and unit variance. This noise is scaled by a constant λ in order to produce perturbations on the synthetic test image. This noise is known as *additive* noise [9]. We decide to use a synthetic image in order to know precisely the location of the corners. The signal-to-noise ratio (SNR) is computed in decibels (DB). Figure 1, shows the structures (a), (b) and (c) with the Gaussian noise scaled by the factors $\lambda = 20, 40, 80$. The test of our L-corner detector considering three optimization algorithms was built as follows:

1. The *Down Hill Simplex*, *Simulated Annealing* and *Evolutionary Algorithm* were applied to the structures (a), (b) and (c) of Figure 1. Those structures show three different corners: straight angle corner, acute angle corner and obtuse angle corner respectively.
2. The size of the window is 13×13 pixels, centered around the pixel:
 - (a) $(u_0, v_0) = (87, 87)$.
 - (b) $(u_0, v_0) = (707, 353)$.
 - (c) $(u_0, v_0) = (396, 397)$.
3. The control parameters of each algorithm are:
 - *Down Hill Simplex*. Maximal number of movements of the simplex $N = 4500$.
 - *Simulated Annealing*. Initial temperature $T = 1$, size of the equilibrium state $I = 20$, maximal number of iterations $N = 4500$.

- *Evolutionary Algorithm*. Crossover percentage $pc = 0.80$, mutation percentage $pm = 0.05$, convergence percentage $pf = 0.75$, offspring number in the population $P = 22$, maximal number of generations $N = 2000$, approximately equivalent to 4500 movements.

4. 30 samples for each test were performed.
5. Percentage of stop criteria, $ftol = 1 \times 10^{-80}$.

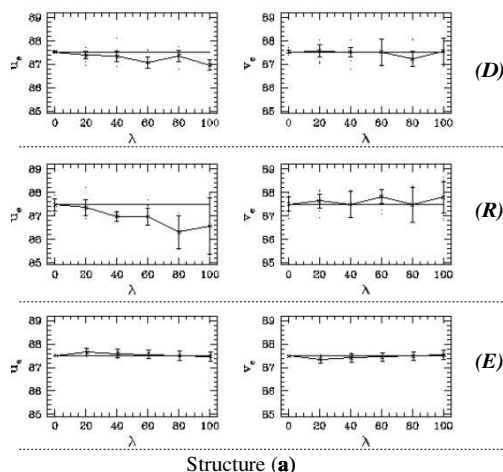


Figure 2: Behaviour of the *Down Hill Simplex* (**D**), *Simulated Annealing* (**R**) and *Evolutionary Algorithm* (**E**) considering a Gaussian noise scaled by a factor λ over the structure (a) of the synthetic image.

As a result of the test the Figures: 2, 3, 4 were generated. These figures show the displacement of the corner position (u_e, v_e) of the structures (a), (b) and (c) respectively, considering that a random Gaussian noise was applied over the test image. Each figure shows the average corner point (\bar{u}_e, \bar{v}_e) and its final standard deviation considering 30 samples for each optimization strategy. The charts on the left of each figure represent the u coordinate and those on the right represent the v coordinate of the image coordinate system (u, v) . The horizontal straight line denotes the corner position (u_e, v_e) of the free-noise synthetic image $\lambda = 0$. After a careful analysis of these figures we conclude the following:

1. Beyond $\lambda = 80$ ($SNR \approx 3.5$), see Figure 2, the contours of the structures (a), (b) and (c) are difficult to be distinguished. However, the random Gaussian noise doesn't blur the borders. Hence, the structure is more or less preserved in shape.

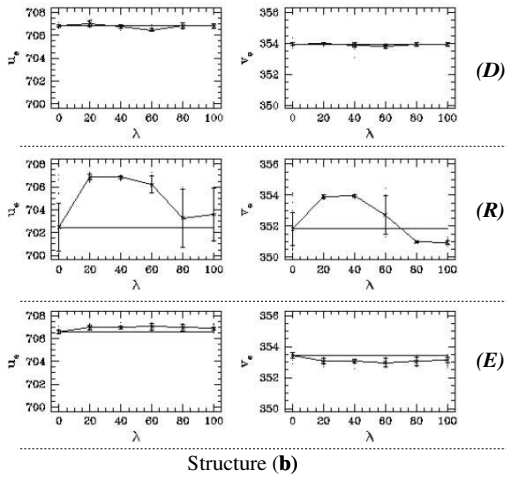


Figure 3: Behaviour of the *Down Hill Simplex* (D), *Simulated Annealing* (R) and *Evolutionary Algorithm* (E) considering a Gaussian noise scaled by a factor λ over the structure (b) of the synthetic image.

2. In the case of structure (a) the *Evolutionary Algorithm* presents the best curve of behaviour in the presence of noise. Moreover, the maximum standard deviation is obtained for $\lambda = 20$. This value is approximately 0.14 pixels.
3. In the case of structure (b) the *Down Hill Simplex* presents the best curve of behaviour in presence of noise. The maximum standard deviation occurs in $\lambda = 60$ over the u axis. This value is about 0.37 pixels compared to 0.47 pixels obtained by the *Evolutionary Algorithm* also in $\lambda = 60$. The curve of the *Evolutionary Algorithm* remains constant around the average value (x_e, y_e) in all cases.
4. In the case of structure (c) the *Evolutionary Algorithm* presents the best curve in presence of noise over the u axis. While, the *Down Hill Simplex* presents the best curve around the v axis.
5. If we observe the error bars representing the standard deviation considering 30 samples for each test we arrive to the following conclusion: 1) The average standard deviation of the *Evolutionary Algorithm* is 0.19, 2) The average standard deviation of the *Down Hill Simplex* is 0.25, 3) The average standard deviation of the *Simulated Annealing* is 0.76 pixels. In summary, the *Evolutionary Algorithm* presents the best average for each experiment.

As a result, the *Evolutionary Algorithm* is less sensitive to noise. Hence, it can be considered more robust. However, the *Down Hill Simplex* offers similar results. Finally,

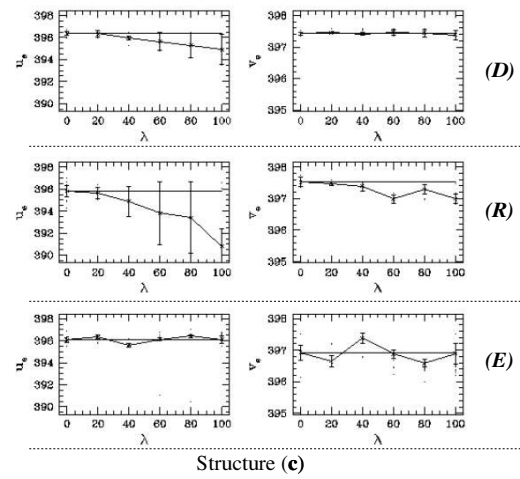


Figure 4: Behaviour of the *Down Hill Simplex* (D), *Simulated Annealing* (R) and *Evolutionary Algorithm* (E) considering a Gaussian noise scaled by a factor λ over the structure (c) of the synthetic image.

the *Simulated Annealing* shows the worst behaviour in the presence of Gaussian noise. The χ^2 value for real images rarely converge to zero. Figure 5, shows an image of an L-corner that presents a set of pixels aligned in a straight line just before making the regular corner. This anomaly produces instability in the algorithms. As a consequence, all algorithms fail at fitting the model to the image data. Maximal machine accuracy used according to IEEE-754 standard is $Res = 1 \times 10^{-16}$, without introducing roundoff errors. Figure 6, shows clearly that this accuracy is achieved before total convergence. Our results about computational time are: The *Down Hill Simplex* requires in average 0.039 seconds for each step, the *Simulated Annealing* requires in average 0.035 seconds in each step and the *evolutionary algorithm* requires in average 0.072 seconds for each generation. However, the heuristic process to generate a solution by the *Evolutionary Algorithm* is 5.1 times faster than the other two. In summary, we obtain a solution between 37 seconds up to 2.5 minutes using a Pentium III 800Mhz.

5. Summary and Conclusions

Accurate L-corner measurement was obtained through a parametric model $M_L'(x, y, \vec{P})$ using an hybrid evolutionary ridge regression approach. The goal was to obtain the best set of parameters $\vec{P} = (\sigma_1, \mu_1, \theta_1, \sigma_2, \mu_2, \theta_2, A, B)$, that fits a window, $2w - 1 \times 2w - 1$, of pixels centered around a pixel (u_0, v_0) within a digital image. Concluding, the *Evolutionary Algorithm* presents the best behaviour against noise. The *Down Hill Simplex* is the simplest strategy to operate because it doesn't requires any control pa-

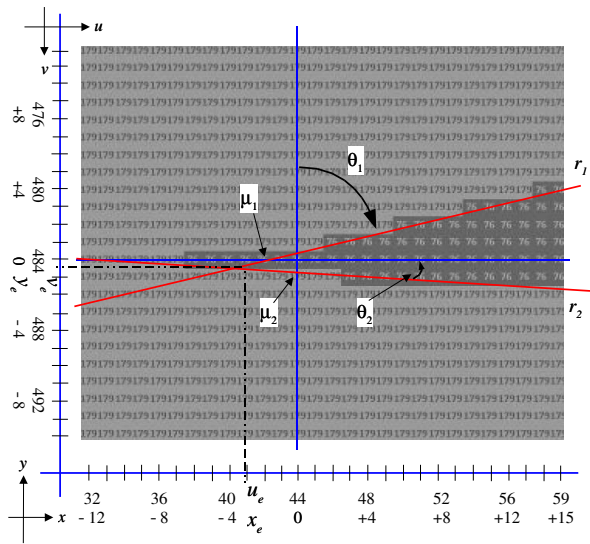


Figure 5: This image shows an example of a corner presenting misleading data.

parameter. On the other hand, the *Evolutionary Algorithm* has the ability to increase the population size, which increases the probability to find a better result in a smaller number of generations.

References

- [1] Ballard, D.H. and Brown, C.M. (1982). *Computer Vision*. Prentice-Hall, Inc., Englewood Cliffs, New Jersey.
- [2] P. Brand and R. Mohr "Accuracy in Image Measure". In Proceedings of the SPIE Conference on Videometrics III, Boston, Massachusetts, USA, Vol. 2350, pp. 218-228, 1994.
- [3] P. R. Beaudet. "Rotationally Invariant Image Operators". IEEE International Conference on Pattern Recognition, pp. 579-583, 1978.
- [4] F. Bergholm. "Edge Focusing". *IEEE Trans. on Pattern Analysis and Machine Intelligence*. Vol 9, pp. 726-741. 1987.
- [5] J. Canny. "A Computational Approach to Edge Detection". *IEEE Trans. on Pattern Analysis and Machine Intelligence*. Vol. 8, No. 6, November, 1986.
- [6] R. Deriche. "Using Canny's Criteria to Derive a Recursively Implemented Optimal Edge Detector". *International Journal of Computer Vision*. pp. 167-187, 1987.
- [7] R. Deriche and G. Giraudon. "Accurate Corner Detection: An Analytical Study". Proc. 3rd Intern. Conf. Comput. Vis., Osaka, December, pp. 66-70. 1990.
- [8] R. Deriche and G. Giraudon. "A Computational Approach for Corner and Vertex Detection". *International Journal of Computer Vision*, 10(2), pp. 101-124, Kluwer Academic Publishers, 1993.
- [9] Dougherty, E. R. (1999). *Random Processes for Image and Signal Processing*. SPIE Optical Engineering Press, and IEEE Press, Inc.
- [10] L. Dreschler and H. H. Nagel (1982). On the Selection of Critical Points and Local Curvature Extrema of Region Boundaries for Interframe Matching. IEEE International Conference on Pattern Recognition, pp. 542-544.
- [11] Faugeras, O. (1996). *Three-Dimensional Computer Vision: A Geometric Viewpoint*. MIT Press, Cambridge, Massachusetts, London, England.

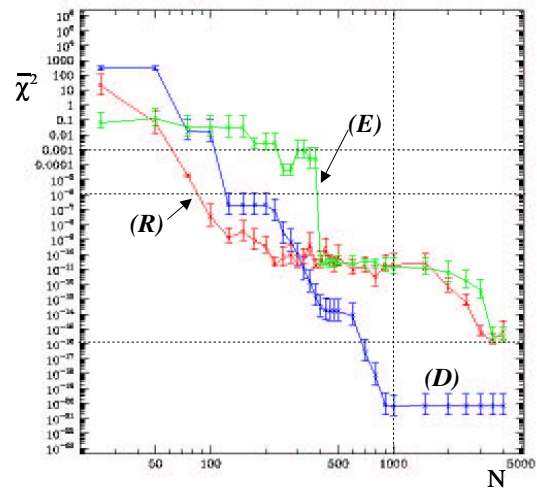


Figure 6: Average computational cost and the corresponding standard deviation measured in number of operations against the χ^2 value both in logarithmic scales.

- [12] A. W. Gruen. "Adaptive Least Squares Correlation: A Powerful Image Matching Technique". *S. Afr. Journal of Photogrammetry, Remote Sensing and Cartography*. 14(3), pp. 175-187. 1985.
- [13] S. Kirkpatrick, C. D. Gelatt, Jr. and M. P. Vecchi. "Optimization by Simulated Annealing". *Science*. Vol. 220, pp. 671-680, 1983.
- [14] L. Kitchen and A. Rosenfeld. "Gray Level Corner Detection". *Pattern Recognition letters*. No. 1, pp. 95-102, 1982.
- [15] G. Olague and B. Hernández. "Flexible Model-based Multi-corner Detector for Accurate Measurements and Recognition". IEEE International Conference on Pattern Recognition, Québec, Canada, Vol. II, pp. 578-583, 2002.
- [16] D. W. Marquardt. "Generalized Inverses, Ridge Regression, Biased Linear Estimation, and Nonlinear Estimation". *Technometrics*. Vol. 12, No. 3, pp. 591-612. August 1970.
- [17] D. Marr and E. Hildreth. "Theory of Edge Detection". *Proc. Roy. Soc. London*, 207, pp. 187-217
- [18] G. Medioni and Y. Yasumoto. "Corner Detection and Curve Representation Using Cubic B-Splines". *Computer Vision, Graphics, And Image Processing*. Vol. 39, pp. 267-278, Academic Press, Inc. 1987.
- [19] H. P. Moravec. "Towards automatic visual obstacle avoidance". In *Proceedings of the 5th International Joint Conference on Artificial Intelligence*, pp. 584, Cambridge, Massachusetts, USA.
- [20] J. A. Nelder and R. Mead. "A Simplex Method for Function Minimization". *Computer Journal*. Vol. 7, pp. 308-313, 1965.
- [21] W. H. Press, B. P. Flanery, S. A. Teukolsky and W. T. Vetterling. "Numerical Recipes in C". Cambridge University Press, Second Edition. 1992.
- [22] K. Rohr. "Modelling and Identification of Characteristic Intensity Variations". *Image and Vision Computing*. Vol. 10, No. 2, March, 1992
- [23] K. Rohr. "Recognizing Corners by Fitting Parametric Models". *International Journal of Computer Vision*. 9(3), pp. 213-230, Kluwer Academic Publishers, 1992.
- [24] D.-M. Tsai, H.-T. Hou and H.-J. Su. "Boundary-based Corner Detection Using Eigenvalues of Covariance Matrices". *Pattern Recognition Letters*. 20, pp. 31-40, Elsevier, 1999.
- [25] Ullman, S. (1996). *High-level Vision*. MIT Press, Cambridge, Massachusetts, London, England.